12WCEE 2000

MOMENTARY ENERGY ABSORPTION AND EFFECTIVE LOADING CYCLES OF STRUCTURES DURING EARTHQUAKES

Yutaka HAGIWARA[1]

SUMMARY

In ultimate-state seismic design, energy input has been used for one of the reliable indices of seismic motions that determine their influences on structural failure and nonlinear response. In this study, a two-term expression of energy input is proposed. The first term, one-cycle momentary energy input, is the work of a seismic motion on structures with the largest one cycle of vibration. The second term, effective loading cycle, is the ratio of total energy input to one-cycle momentary energy input, which is related to the number of load-displacement hysteresis loops of structures during a seismic motion. This new separated expression of energy input can quantify both momentary and cumulative damage potential of seismic motions, and relates them various types of structural failure. To demonstrate the fundamental characteristics and virtues of these two indices, they are applied to spectral analyses of seismic motion records and unified description of energy absorption capacity of structures in dynamic failure tests. Then a generic framework of seismic margin evaluation is proposed being based on the two-term energy expression. This framework is expected to ensure that structures have uniform seismic margin for various seismic motions and various failure modes.

INTRODUCTION

Energy balance of structural capacity and seismic motions is one of the essential bases for modern seismic design of ductile structures. After pioneering work of Housner (1959), Akiyama (1985) systematically developed seismic design methodologies based on total energy input, which represents cumulative dissipated energy by structures during a seismic motion. After the occurrence of the 1995 Hyogoken-nanbu earthquake in Japan, various researches have been conducted on structural failure caused by seismic motion with very short duration. Consequently, momentary aspect of energy of seismic vibration has been emphasized. However, both first-passage failure and cumulative failure can occur during earthquakes depending on structural types, functions, and seismic motion characteristics. Momentary energy quantifies destructive potential of seismic motions only for first-passage failure. Generalized measures for seismic influences are expected, which can be applied for any failure modes and any types of seismic motions.

In this study, a two-term expression of total energy input is proposed. The first term, one-cycle momentary energy input, is energy absorbed by structures during one cycle of vibration, which governs first-passage failure. The second term, effective loading cycles, is the ratio of total energy input to one-cycle momentary energy input, which determines cumulative failure in combination with the first term. These indices can separately quantify momentary and cumulative damage potential of seismic motions, and relate them to various structural failures.

This paper is composed of four parts. At first, the two-term expression of energy input is defined. Then, it is applied to spectral analyses of seismic motion records and its fundamental characteristics are illustrated. It is also applied to unified description of energy absorption capacity of structures in the seismic buckling tests of cylindrical shells. Finally, a generic framework of seismic margin evaluation is presented being based on the proposed energy indices.

[1] *Abiko Research Lab, Central Research Institute of Electric Power Industry, Japan, Email:hagiwara@criepi.denken.or.jp*

DEFINITIONS

Total Energy Input

Akiyama (1985) defined total energy input as cumulative dissipated energy by structures during a seismic motion, and applied it for ultimate-state seismic design of structures. For the definition, inelastic response of a single-degree-of-freedom (SDOF) system is assumed by Eq. (1).

$$m\ddot{x} + c\dot{x} + F(x) = -m\ddot{x}_g \tag{1}$$

where, x: relative displacement, m: mass, c: viscous damping coefficient, $F(x)$: restoring force, $\ddot{x}_g$: acceleration of ground motion. By integrating Eq. (1) multiplied by displacement increment, $\dot{x}dt$, for the duration of seismic motion, t_0, the energy balance equation Eq. (2) is derived.

$$\int_0^{t_0} m\ddot{x}\dot{x}dt + \int_0^{t_0} c\dot{x}^2 dt + \int_0^{t_0} F(x)\dot{x}dt = -\int_0^{t_0} m\ddot{x}_g \dot{x}dt \tag{2}$$

The total energy input E, the right-hand side of Eq. (2), and its equivalent velocity V_E are defined by Eq. (3).

$$E = -\int_0^{t_0} m\ddot{x}_g \dot{x}dt\ ,\ V_E = \sqrt{2E/m} \tag{3}$$

Energy spectrum $S_{VE}(T,\ h)$ is the spectrum of V_E for linear SDOF systems whose natural period and damping are denoted by T and h. The total energy input can represent cumulative load effect of seismic motions in a simplified and unified form. However, the total energy input has due dependency on the duration of seismic motions, and it cannot express the difference in load effect between large-amplitude/short-duration seismic motions and small-amplitude/long-duration ones. This makes problems in evaluating comprehensive seismic margin of structures for various seismic motions that have variety of duration, which is essentially important in the seismic design of nuclear power stations.

One-Cycle Momentary Energy Input

In order to deal with the problems of the total energy input, the author defined the one-cycle momentary energy input $\Delta_1 E\ (t)$ by Eq. (4), which means energy input for one-cycle of vibration [Hagiwara, 1992a].

$$\Delta_1 E(t) = -\int_{t-T}^{t} m\ddot{x}_g \dot{x}dt \tag{4}$$

where T : natural period in linear systems or effective response period in nonlinear systems. One-cycle momentary energy input can be interpreted as time history of energy input observed by a sliding time window that has width T. Though, similar expressions on momentary energy input have been proposed by various authors [e.g. Akiyama and Miyazaki, 1989. Ohi et al., 1991. Nishizawa and Kaneta, 1991. Kuwamura et al., 1997], the above-stated expression has advantages in clear relations to load-displacement hysteresis loops of structures during earthquakes. When $\Delta_1 E_m$ denotes the maximum value in a time history of $\Delta_1 E(t)$ at the time t_m, its equivalent velocity $\Delta_1 V_E$ is defined by Eq. (5).

$$\Delta_1 V_E = \sqrt{2\Delta_1 E(t_m)/m} = \sqrt{2\Delta_1 E_m/m} \tag{5}$$

The one-cycle momentary energy input represents the maximum momentary load effect of seismic motion. In this expression, the effect of the duration and phase content is excluded. $S_{\Delta 1VE}(T,\ h)$ is equivalent velocity spectrum of one-cycle momentary energy input $\Delta_1 V_E$ for linear SDOF systems. Obviously, $S_{\Delta 1VE}$ is closely related to velocity spectrum S_V. For floor response of nuclear reactor building, an empirical rule shown in Eq. (6) can be applied when damping factor h is 0.05 or larger.

$$S_{\Delta 1VE}/S_V \approx \sqrt{0.4 + 4\pi h} \tag{6}$$

Effective Loading Cycles

The ratio of total energy input to one-cycle momentary energy input is related to the number of load-displacement hysteresis loops of structures during earthquakes. In this study, the effective loading cycle N_E and their spectra S_{NE} are defined by Eq. (7) [Hagiwara, 1992b], which represents duration and phase-content.

$$N_E = E/\Delta_1 E_m = \left(V_E/\Delta_1 V_E\right)^2,\ S_{NE} = \left(S_{VE}(T,h)/S_{\Delta 1VE}(T,h)\right)^2 \tag{7}$$

Two-term Expression of Energy Input

Figure 1 shows a conceptual view of total energy input, one-cycle momentary energy input, and effective loading cycle. Total energy input corresponds to cumulative absorbed energy of a structure during an earthquake with multiple cycles of hysteresis. One-cycle momentary energy input is related to the energy absorbed by the largest one cycle of hysteresis. Effective loading cycles are related to numbers of hypothetical hysteresis loops when total energy input is absorbed by repetition of the largest cycle.

In this study, a new two-term expression is proposed for energy input, which uses one-cycle momentary energy input and effective loading cycles. In the proposed expression, damage potential of a seismic motion is described by the clearly separated two terms which represent momentary large amplitude and phase/duration aspects, respectively. Both terms are intuitively and quantitatively related to actual response and damage of structures. The proposed expression can characterize the difference of various seismic motions (e.g. large-amplitude/short-duration motions and small-amplitude/long-duration motions), and can relate them to various failure modes (e.g. impulsive first-passage failure and cumulative failure).

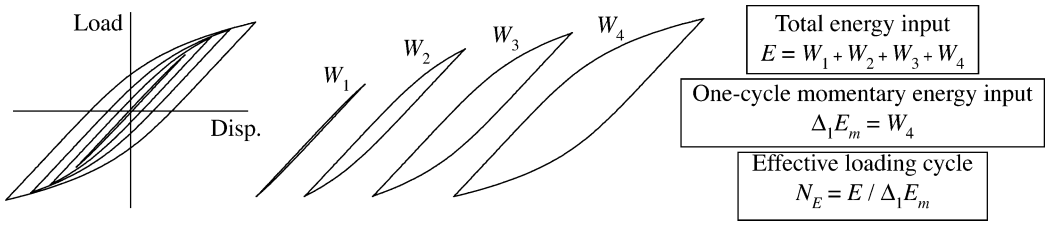

Figure 1: Conceptual view of the two-term expression of energy input

ENERGY SPECTRA OF STRONG MOTION RECORDS

For strong ground motion records shown in Table 1 and Fig. 2, spectra for total energy input S_{VE} (Fig. 3a), one-cycle momentary energy input $S_{\Delta 1VE}$ (Fig. 3b), and effective loading cycles S_{NE} (Fig. 3c) were computed in order to demonstrate fundamental nature of the proposed expression [Hagiwara and Yabana, 1996]. The damping factors are 0.10 in all spectra.

These spectra clearly characterize the difference of the seismic motions in several important aspects of earthquake-proof design. The largest total energy input is observed in KUS/93, which have the largest amplitude and relatively longer duration (Fig. 3a). The largest one-cycle momentary energy input is observed in KOB/95 which is widely known as impulsive large amplitude and devastating damage in a few cycles of vibration (Fig. 3b). The spectra of effective loading cycles are expected to have close correlation with duration of seismic motions and magnitude of earthquakes. The seismic motions caused by larger events, KUS/93 and NMR/94, show larger values on the effective loading cycles compared to the others, as expected (Fig. 3c).

Table 1: Seismic ground motions for spectral analysis

Name	Earthquake	Magnitude	Component	Observatory	Hypocentral Distance
KUS/93	1993 Kushiro-oki	7.8	EW	Kushiro /JMA	111.6 km
HAC/94	1994 Sanriku-haruka-oki	7.5	NS	Hachinohe /JMA	204.5 km
NMR/94	1994 Hokkaido-toho-oki	8.1	NS	Nemuro /CRIEPI	171.0 km
KOB/95	1995 Hyogoken-nanbu	7.2	NS	Kobe /JMA	25.5 km

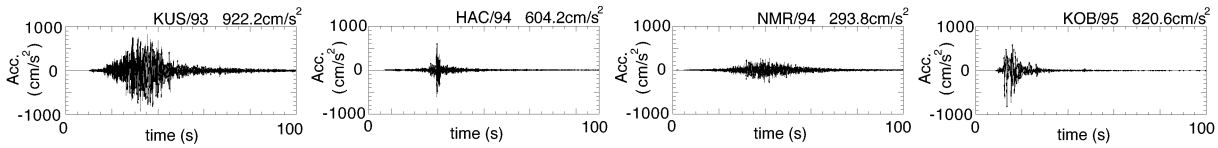

Figure 2: Acceleration records of seismic ground motions

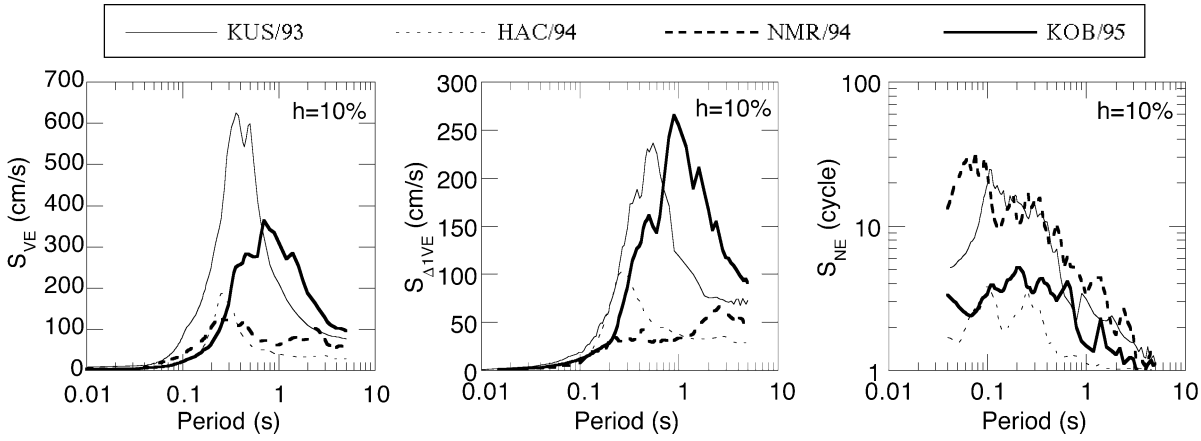

(a) Total energy input (b) One-cycle momentary energy input (c) Effective loading cycle

Figure 3: Spectral analysis of seismic ground motions

APPLICATION TO SEISMIC BUCKLING TESTS OF CYLINDRICAL SHELLS

Seismic Buckling Tests of Cylindrical Shells

Though "energy absorption capacity" is often evaluated in seismic tests of structures, its comparison has been difficult because of ambiguous definition. The proposed two-term expression of energy input provides a unified way to quantify and to compare energy absorption capacities under various conditions. The author conducted shaker table tests (Fig. 4) and pseudo-dynamic tests (Fig. 5) of cylindrical shells in order to study inelastic post-buckling behavior during earthquakes [Hagiwara, 1993, 1995, 1999]. The test apparatuses were simple nonlinear SDOF systems. The test models were cylindrical shells made of stainless steel or aluminum alloy, which were subjected to transverse shearing load induced by horizontal seismic excitation. The tests were performed for various test models and various seismic motions in order to prepare the seismic design guidelines for fast breeder reactors. Two seismic motions, ENVELOPE and FR4, were used for the excitations in the shaker table tests (Fig. 6. Amplitude and duration of the seismic motions are scaled up/down in the tests). The longer motion, ENVELOPE, is a simulated floor response for a reactor building which is partially embedded in hard rock. The shorter one, FR4, is also a simulated floor response for a reactor building mounted on surface of relatively soft rock. Horizontal transverse shearing load and horizontal displacement at loading point of the cylindrical shells were acquired for the shaker table tests. Figure 7 shows the load-displacement relations induced by ENVELOPE and FR4 for the cylinders that have same specifications (Material: aluminum alloy A3003P-O, radius-to-thickness ratio: 100, length-to-radius ratio: 1.5, loading-height-to-radius ratio: 2.14). By comparing two test results in Fig. 7, considerable differences are observed especially for the numbers of the load-displacement loops, though the skeleton curves are virtually the same. The difference of ENVELOPE and FR4 in duration and phase-content is the dominant cause of these results, resulting in apparent difference in total energy absorption during an excitation.

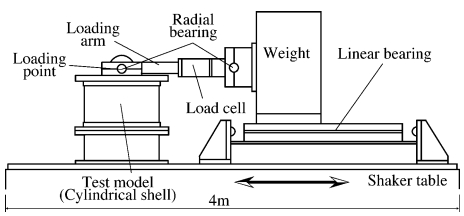

Figure 4: Shaker table test apparatus

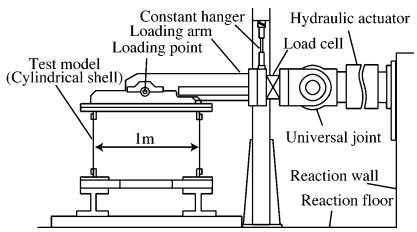

Figure 5: Pseudo-dynamic test apparatus

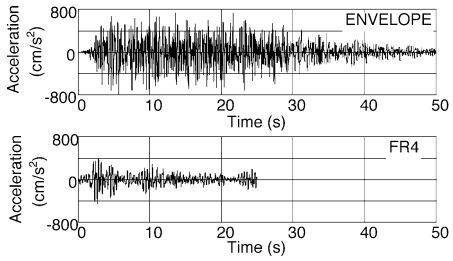

Figure 6: Seismic excitations on the shaker table

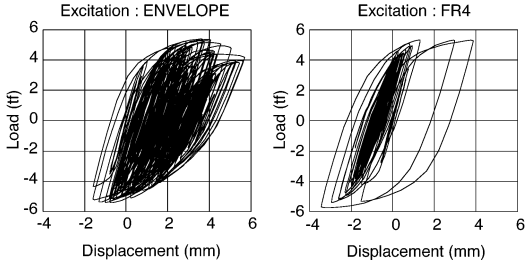

Figure 7: Load-displacement relations

Energy Absorption

The energy absorption E_D and its normalized equivalent velocity V_D/V_e can be computed by Eq. (8) for any seismic responses.

$$E_D = \sum_t \Delta Q \cdot \Delta\delta \ , \ V_D/V_e = \sqrt{E_D/E_e} = \sqrt{E_D/(Q_{cr}\delta_e/2)} \tag{8}$$

where, ΔQ and $\Delta\delta$ are load and displacement increment during a time step, respectively. E_e and V_e are maximum elastic vibration energy and its equivalent velocity defined by Eq. (9) (Fig. 8).

$$E_e = Q_{cr}\delta_e/2 \ , \ V_e = \sqrt{2E_e/m} \tag{9}$$

where, Q_{cr} is buckling load, δ_e is displacement for pseudo linear limit ($\delta_e = Q_{cr}/k_0$, k_0 :initial stiffness).

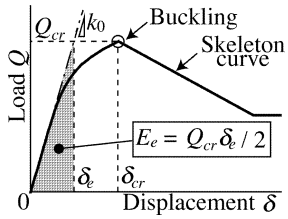

Figure 8: Maximum elastic vibration energy

Figure 9 shows $V_D/V_e - \delta_{\max}/\delta_e$ relations ($\delta_{\max}$: maximum displacement) for the shaker table tests and the pseudo-dynamic tests of the cylindrical shells. Each marker in Fig. 9 corresponds to a shake in a test. The names appeared in the legend mean the seismic motions applied in the tests, and they are grouped according to duration and dominant period, as follows.

i) Marker ○ : CONST, TK4, ENVELOPE
- Long duration (40~50s. Cut down to 10~20s in several cases), short dominant period (0.2s)
- Floor response of half-embedded reactor building in relatively hard lock.

ii) Marker ● : FR4
- Short duration (25s), relatively long dominant period (0.4s)
- Floor response of surface-mounted reactor building on relatively soft lock.

iii) Marker × : AMS2X7
- Long duration (40s), extremely long dominant period (1.5s)
- Floor response of seismic-isolated reactor building.

Though the energy absorption shows correlation with the displacement on Fig. 9, the markers are considerably scattered and the three groups show apparently different trends. One of the causes must be the difference of duration or number of loading cycles. The other cause seems to be the asymmetry of load-displacement loops with respect to displacement. These results clarify that there exist some difficulties in evaluating energy absorption capacity with a unified reference.

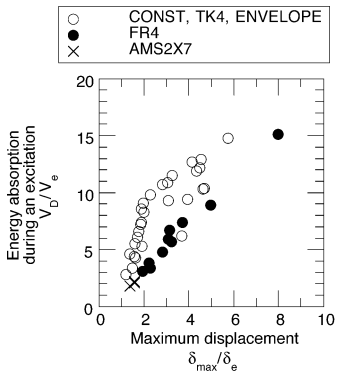

Figure 9: Energy absorption during an excitation

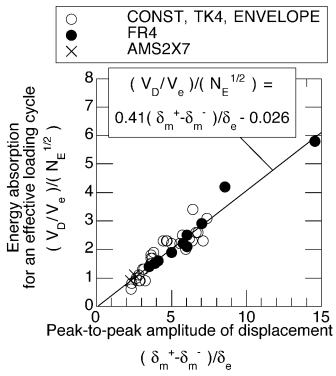

Figure 10: Energy absorption for an effective loading cycle

Momentary Energy Absorption

The first cause of the scattered markers in Fig. 9 can be eliminated by use of the proposed two-term expression of energy input. The second cause can be avoided by plotting energy absorption against peak-to-peak amplitude of displacement ($\delta_m^+ - \delta_m^-$), where δ_m^+ and δ_m^- are the largest positive displacement and the largest negative displacement, respectively. Assuming effective loading cycles N_E of nonlinear systems are equivalent to the spectra of effective loading cycles S_{NE} at effective response period T_e for damping factor 10%, the energy absorption for one-cycle of vibration, E_D/N_E, and its equivalent velocity can be predicted by Eq. (10). These expressions give a unified way to define one-cycle momentary energy absorption capacity of structures, which is independent from duration or phase-content of seismic motions.

$$E_D/N_E \approx E_D/S_{NE}(T_e), \quad (V_D/V_e)/\sqrt{N_E} \approx (V_D/V_e)/\sqrt{S_{NE}(T_e)} \tag{10}$$

The effective response period T_e for nonlinear systems can be estimated by Eq. (11) [Akiyama, 1985].

$$T_e = \sqrt{(T_0^2 + T_0 T_m + T_m^2)/3}, \quad T_m = T_0\sqrt{k_0/\{(Q_m^+ - Q_m^-)/(\delta_m^+ - \delta_m^-)\}} \tag{11}$$

where, Q_m^+ and Q_m^- are loads when δ_m^+ and δ_m^- observed, respectively. T_m is estimated maximum response period. Figure 10 shows the relations between energy absorption for an effective loading cycles and peak-to-peak amplitude of displacement in the shaker table tests and the pseudo-dynamic tests. Figure 10 shows the good correlation between the energy absorption for an effective loading cycle and peak-to-peak amplitude of displacement. The regression curve on Fig. 10, Eq. (12), characterizes the essential performance of the cylindrical shells in terms of dynamic ductility.

$$(V_D/V_e)/\sqrt{N_E} = 0.41(\delta_m^+ - \delta_m^-)/\delta_e - 0.026 \tag{12}$$

For any structures, appropriate seismic tests or analyses can be applied to determine such curves, which would be convenient for comparisons of energy absorption, because results obtained by various seismic motions can be compared each other with a unified reference. However, it should be noted that such curves only give a function between displacement and one-cycle momentary energy absorption. In order to define "energy absorption capacity" for ultimate state, it is necessary to define a corresponding limit, as shown in next chapter.

FRAMEWORK OF SEISMIC MARGIN EVALUATION

In this study, "Seismic Margin f " means the ratio of the seismic motion amplitude that causes ultimate state to the amplitude for design conditions. The ultimate state of a structure can be given by a function of one-cycle momentary energy absorption capacity and effective loading cycles, as shown in Fig. 10 and Eq. (12). On the other hand, the influence of earthquakes can be determined by the spectra of the two-term expression of energy input for the seismic motions expected on a site.

The seismic margin of structures can be visualized by drawing the relations between the one-cycle momentary energy input and the effective loading cycles, as shown in Fig. 11. On Fig. 11, the ultimate state is shown by a continuous curve, which is declined to the right because cumulative damage is assumed. Influence of a seismic motion is shown by a marker (outlined circle) which corresponds to a set of values on the two spectra $S_{\Delta 1VE}$ and S_{NE} at T_e for the ultimate state. Small nearfield earthquakes and large interplate earthquakes will appear on the plot at its left side and its right side, respectively. The collective influence of earthquakes expected on a site will be defined by the upper bound of a group of markers. The distance of the upper bound of earthquake markers and the ultimate state curve determines the seismic margin f. In a particular case when ultimate state is defined by first-passage failure of a displacement or a ductility factor, a horizontal line on Fig. 11 will define the ultimate state, then the seismic margin f can be computed by Eq. (13)[Hagiwara, 1999].

$$f = \left(V_D / \sqrt{N_E} \right) / S_{\Delta 1VE} \tag{13}$$

With this framework, seismic margin of structures can be evaluated by a unified approach. It can give structures uniform margin for various seismic motions (e.g. large-amplitude/short-duration motions and small-amplitude/long-duration ones) and various failure modes (e.g. impulsive failure and cumulative failure).

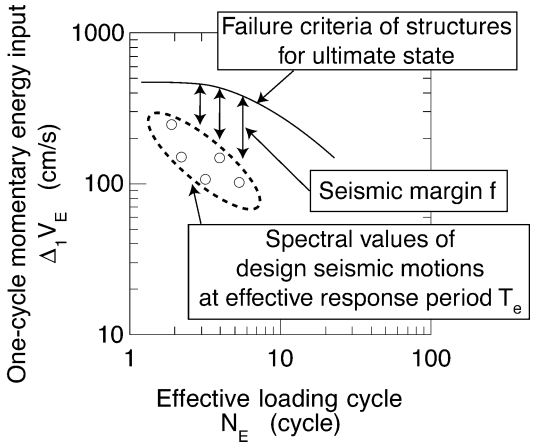

Figure 11: Concept of the seismic margin evaluation

6. CONCLUSIONS

A two-term expression of energy input is proposed for flexible and unified description of seismic influences on structures. The first term, one-cycle momentary energy input, is the energy input caused by the largest one-cycle of vibration, and corresponds to the largest hysteresis loop of load-displacement relations of structures. The second term, effective loading cycles, is the ratio of total energy input to one-cycle momentary energy input, which is related to the number of hysteresis loops during an earthquake. These indices can separately quantify momentary and cumulative damage potential of seismic motions, and relate them to various structural failures.

To demonstrate the fundamental characteristics of proposed expression, it was applied to spectral analyses of seismic ground motions. The results proved ability of proposed expression to characterize profiles of seismic motions in both momentary large amplitude and its repetition. The proposed method was also applied to data analyses of seismic buckling tests of cylindrical shells. The results of the analyses suggested that one-cycle momentary energy input could be used as a unified and common reference of structural energy absorption capacity, even though those data were obtained from tests for various seismic motions that had different spectral profiles and phase-content.

Finally, a generic framework of seismic margin evaluation was proposed being based on the proposed expression. This framework is expected to ensure that structures have uniform seismic margin for various seismic motions and various failure modes.

ACKNOWLEDGMENT

The seismic buckling tests on cylindrical shells were conducted as a part of “Verification Tests of Fast Breeder Reactor Technology” sponsored by Ministry of International Trade and Industry.

REFERENCES

Akiyama, H. (1985), *Earthquake Resistant Limit-State Design for Buildings*, University of Tokyo.

Akiyama, H. and Miyazaki, M. (1989), “Response Prediction based on increment of energy input”, *Recommendation for the Design of Base Isolated Buildings - Commentary*, Architectural Institute of Japan, pp88-92.

Hagiwara, Y. and Yamamoto, K. (1992a), *A Seismic Margin Evaluation Method of Steel Cylindrical Shells Based on Energy Input during 1-Cycle of Vibration*, CRIEPI Report No. U91055.

Hagiwara, Y. (1992b), *Energy Input Characteristics of Seismic Motions during 1-Cycle of Vibration and the Seismic Margin Evaluation Method with the Consideration on Cumulative Damage*, CRIEPI Report No. U92032.

Hagiwara, Y. et al. (1993), “Dynamic Buckling and Nonlinear Response of Fast Breeder Reactor Main Vessels under Earthquake Loading”, *JSME International Journal*, Series B, Vol. 36, No. 3, pp476-484.

Hagiwara, Y. et al. (1995), “Dynamic Shear-Bending Buckling Experiments of Cylindrical Shells”, *Transactions of the 13th International Conference on Structural Mechanics in Reactor Technology*, Vol. E, pp469-474.

Hagiwara, Y. and Yabana, S. (1996), “Characteristics of the Main Shock Seismogram Viewed from Energy Input”, *General Report on Investigations of Fault, Earthquake Motion and Damage due to The 1995 Hyogoken-nanbu Earthquake*, CRIEPI General Report No. U29, pp64-71.

Hagiwara, Y. (1999), *Studies on Shear-Bending Buckling under Elastic-Plastic Seismic Response for Cylindrical Main Vessels of Fast Breeder Reactors*, Doctoral Thesis, University of Tokyo.

Housner, G. W. (1959), “Behavior of Structures during Earthquakes”, *Journal of Engineering Mechanics, Proceedings of ASCE*, EM4, pp109-129.

Kuwamura, H. et al. (1997), “Energy Input Rate in Earthquake Destructiveness – Comparison between Epicentral and Oceanic Earthquakes”, *Journal of Structural and Construction Engineering*, No. 491, Architectural Institute of Japan, pp29-36.

Nishizawa, H. and Kaneta, K. (1991), “On the Energy Response of Single Degree of Freedom System Subjected to an Intense Earthquake Part. I. On-line Simulation of Steel and Reinforced Concrete Models”, *Journal of Structural and Construction Engineering*, No. 424, Architectural Institute of Japan, pp117-124.

Ohi, K. et al. (1991), “Energy Input Rate Spectra of Earthquake Ground Motions”, *Journal of Structural and Construction Engineering*, No. 420, Architectural Institute of Japan, pp1-7.